Optoacoustic monitoring of real-time lesion formation during radiofrequency catheter ablation

Genny A. Pang [a,b], Erwin Bay [a,b], Xosé Luis Deán-Ben [a], Daniel Razansky* [a,b]
[a] Institute for Biological and Medical Imaging (IBMI), Helmholtz Center Munich, Ingoldstädter Landstraße 1, 85764 Neuherberg, Germany; [b] Faculty of Medicine, Technical University of Munich, Ismaninger Straße 22, 81675 Munich, Germany

ABSTRACT

Current radiofrequency cardiac ablation procedures lack real-time lesion monitoring guidance, limiting the reliability and efficacy of the treatment. The objective of this work is to demonstrate that optoacoustic imaging can be applied to develop a diagnostic technique applicable to radiofrequency ablation for cardiac arrhythmia treatment with the capabilities of real-time monitoring of ablated lesion size and geometry. We demonstrate an optoacoustic imaging method using a 256-detector optoacoustic imaging probe and pulsed-laser illumination in the infrared wavelength range that is applied during radiofrequency ablation in excised porcine myocardial tissue samples. This technique results in images with high contrast between the lesion volume and unablated tissue, and is also capable of capturing time-resolved image sequences that provide information on the lesion development process. The size and geometry of the imaged lesion were shown to be in excellent agreement with the histological examinations. This study demonstrates the first deep-lesion real-time monitoring for radiofrequency ablation generated lesions, and the technique presented here has the potential for providing critical feedback that can significantly impact the outcome of clinical radiofrequency ablation procedures.

Keywords: radiofrequency, cardiac ablation, optoacoustic, photoacoustic, tomography, real-time, three-dimensional, lesion monitoring

1. INTRODUCTION

Non-invasive imaging guidance of radiofrequency ablation (RFA) in cardiac muscle tissue could lead to large improvements in the efficacy and safety of RFA treatments of atrial fibrillation (AF), the most common type of cardiac arrhythmia with currently more than a projected 2 million cases[1]. A non-negligible number of RFA procedures still require retreatment to successfully eliminate AF reoccurrence[2], a problem that is present, in part, because no such direct imaging capability exists to monitor lesion formation in real time during clinical treatment. While continuously improving technologies have led to corresponding improvements of RFA success rates in recent history, there is still a need to reduce the number of post-RFA arrhythmia reoccurrences.

Different imaging modalities have previously been suggested for monitoring of RFA lesion formation. Advances in magnetic resonance imaging (MRI) technology have led to MRI-based techniques for ex vivo visualization of RFA lesion formation in real time[3]. However, temporal and spatial resolution using MRI are limited, and the high costs of operation and specialized equipment prohibit MRI-based techniques from becoming commonplace in regular clinical treatments of RFA. Pure pulse-echo ultrasound methods have been proposed to detect RFA lesion depth progression in real time[4], but yield poor imaging contrast and difficulties in clearly distinguishing the ablated lesion boundary. Novel ultrasound-based methods[5,6] attempt to improve the lesion contrast in RFA monitoring; however, these techniques still fall short of providing direct lesion imaging with good temporal resolution. Optical imaging techniques[7] have been suggested to be capable of real-time monitoring of RFA lesion formation with high spatial resolution, although the penetration depth of pure optical imaging techniques is not sufficient for feedback sensing in RFA procedures for arrhythmia treatment.

* dr@tum.de; phone +49-(0)89-3187-1587; fax +49-(0)89-3187-3063;

Photons Plus Ultrasound: Imaging and Sensing 2015, edited by Alexander A. Oraevsky, Lihong V. Wang
Proc. of SPIE Vol. 9323, 932308 · © 2015 SPIE · CCC code: 1605-7422/15/$18
doi: 10.1117/12.2079704

Optoacoustic imaging, a hybrid imaging technique combining optics and ultrasound, can potentially overcome both the contrast limitation of pure ultrasound detection and the diffusion-limited penetration depth of pure optical imaging. Ablated and unablated tissue have been shown to have distinct optoacoustic spectra[8], yet implementation of optoacoustic imaging for monitoring lesion formation during RFA in real time has not been reported. In the current work, we demonstrate that optoacoustic tomography is capable of real-time three-dimensional imaging of RFA lesion generation, attaining excellent contrast between necrotic and unablated tissue.

2. METHODS

2.1 Experimental methods

Figure 1 presents a schematic of the experimental setup that enabled real-time optoacoustic monitoring during the radiofrequency ablation of ex vivo tissue samples. Optoacoustic excitation was achieved with an optical parametric oscillator (OPO) laser source (Phocus, Opotek Inc., Carlsbad, California USA) capable of generating nanosecond-duration pulses in the wavelength range between 700 nm to 900 nm. The illumination is directed toward the tissue using a custom made silica fused-end fiber bundle (CeramOptics GmbH, Bonn, Germany). The laser power was adjusted such that the fluence rate at the tissue surface was approximately 20 mJ/cm^2 in accordance with safety standards[9]. Acoustic detection was performed with a custom-made optoacoustic probe with a matrix ultrasonic array (Imasonic SaS, Voray, France) consisting of 256 elements distributed on a spherical surface with 40 mm radius. More details on the acoustic detector array can be found elsewhere[10]. The acoustic signals were recorded with a custom designed multi-channel data acquisition system (Falkenstein Mikrosysteme GmbH, Taufkirchen, Germany).

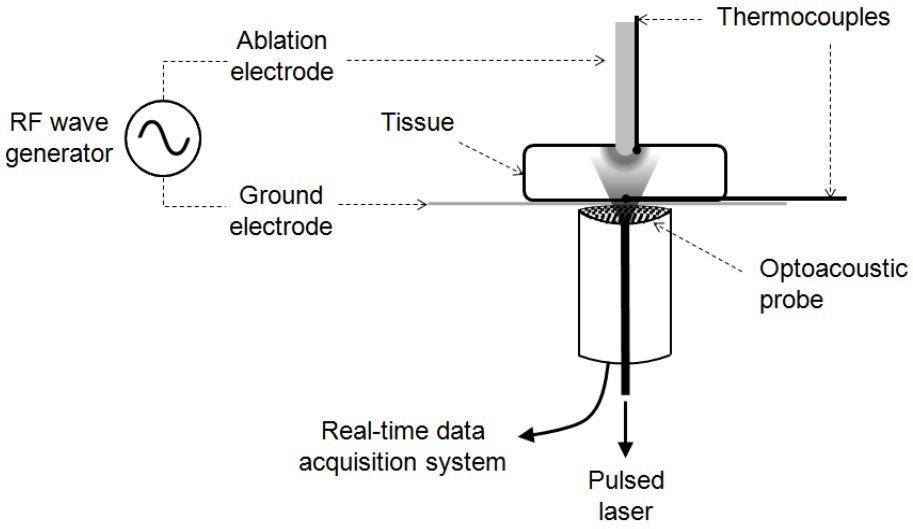

Figure 1. Schematic illustrating the experimental setup of the optoacoustic imaging method and radiofrequency ablation.

Fresh porcine hearts excised shortly before the experiment were used for illustrating the optoacoustic RFA monitoring capabilities. Segments of homogeneous ventricular myocardial tissue of a thickness of approximately 6 mm were excised with a clean scalpel before placement in the ablation and optoacoustic experimental setup. Radiofrequency ablation was performed using a 3 mm diameter ablation electrode with the tip of the ablation electrode positioned approximately at the center of the spherical array of the optoacoustic probe. The tissue sample to be ablated is situated under the ablation electrode, and acoustically coupled to the optoacoustic probe with a 20 mm thick layer of agar gel. A ground electrode of 20 cm^2 in surface area was fabricated with an aperture in the center to allow sufficient light to pass through and illuminate the tissue sample and placed in the volume of agar gel near the fiber output. The tissue sample and the ablation electrode were submerged in solution during ablation for heat dissipation. Temperature was measured

continuously during ablation at the tip of the ablation electrode and at the illuminated surface of the tissue sample using miniature type-T thermocouples (Physitemp Instruments Inc., Clifton, New Jersey USA) with a diameter of 0.41 mm.

In each experiment, ablation was carried out for 60 seconds at a steady-state power of approximately 5 W. The ablation power was adjusted to maintain a temperature of 75°C at the surface of the ablation electrode. During each ablation experiment, the optoacoustic signals excited by a fixed illumination wavelength were simultaneously recorded for all 256 tomographic locations at a frame rate established by the pulse repetition frequency of the laser (10 Hz). After completion of the ablation process, the tissue sample was allowed to cool to room temperature (25°C) and additional optoacoustic measurements were taken to record the final state of the lesion. After the completion of the experiment, the ablated samples were sectioned with a clean scalpel and inspected visually.

2.2 Image reconstruction methods

Three-dimensional optoacoustic images were obtained from the measured data by first applying a band-pass-filter to the signals between 0.1 and 3 MHz to remove low frequency offsets, high frequency noise, and reconstruction artifacts, and then subsequently using a model-based inversion technique with good quantitative performance to render the images[11]. This image reconstruction technique assumed a homogenous speed of sound distribution in the medium, empirically set to 1540 m/s based on the corresponding speed of sound values of soft tissue and agar. While considerable temperature increase occurs during ablation in the treated tissue volume and leads to changes in the speed of sound, a constant value of the speed of sound was used here in all reconstructions because the heat affected zone is relatively small and the agar gel, remaining near room temperature during the entire ablation process, constitutes the vast majority of the acoustic propagation volume. Thus, errors in the reconstructed position due to temperature-induced speed of sound variations are expected to be negligible.

The reconstructed optoacoustic images were corrected for optical attenuation by assuming the light fluence along the axial direction follows an exponential fluence decay function. This exponential function correction also corrects for detector sensitivity influences in the reconstructed image. The rate of exponential decay was determined empirically based on the measured axial decay in optoacoustic image for the intact tissue sample (assumed uniform) before the start of the ablation experiment.

3. RESULTS

3.1 Static lesion visualization

Figure 2 shows a maximum amplitude projection through lateral planes of the reconstructed volume from a representative imaging experiment performed at 860 nm. Figures 2(A) and (B) show the images before and after ablation, respectively, both at room temperature. A uniform region of optoacoustic signal is seen from the tissue volume in the pre-ablation image, indicating a quantitatively accurate fluence decay correction. Two areas of distinct optoacoustic signal strengths can be seen in the tissue sample in the post-ablation image, representing damaged and non-damaged tissue. Three distinct interfaces in the signal are clearly visible separating areas of different optoacoustic signal intensity. These interfaces are, from top to bottom: (1) the interface between the electrode and the tissue sample, (2) a boundary between a region of high optoacoustic signal and a region of lower signal within the tissue sample, and (3) the interface that marks the boundary of the illumination side surface of the tissue sample. The fluence decay correction in the volume of the ablated tissue should not necessarily be the same as in the unablated tissue volume because of changes in optical properties of the damaged tissue, and a non-uniform fluence correction in the axial direction could be used after lesion formation begins. However, for practical purposes of visualizing the lesion boundary, the constant fluence decay correction approximation was applied here.

Figure 2(C) presents a photograph of a cross-sectional view of the lesion obtained with scalpel cut along its central region. The lesion appearance contains three distinct regions, one highly coagulated region close to the ablation electrode tip (darker with more of a brownish appearance), a less coagulated region (lighter with more of a whitish appearance), and the unablated tissue (reddish). There is a slight discrepancy in the imaged and photographed tissue thickness due to the fact that the thickness of the sample is reduced when compressed under the ablation electrode. A 25% compression of the total tissue thickness is observed in the current case, which is reasonable to expect from compression due to electrode placement. The depth of the visualized lesion is measured in the reconstructed image in Figure 2(B) as 1.2 mm; if one assumes a uniform compression of the sample by the electrode, and thus a uniform expansion of the tissue in the post-

ablation sample analysis, the lesion interface in the image can be assumed to represent the boundary of the highly coagulated tissue volume which extends to a depth of 1.6 mm below the electrode in the cross-sectional photograph of a sliced specimen as in Figure 2(C).

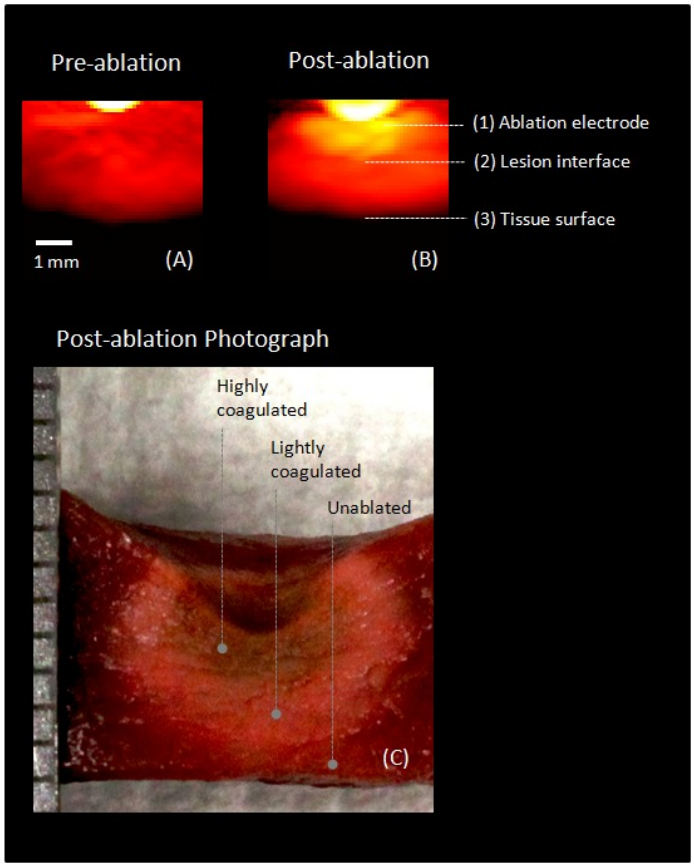

Figure 2. (A) Pre-ablation and (B) post-ablation maximum amplitude projection (MIP) through the lateral planes of the fluence-corrected 3D optoacoustic image reconstructions taken from a representative tissue sample at 25°C with illumination wavelength of 860 nm. Scale bar representing 1 mm in both images is shown. (C) Cross-sectional photograph taken after completion of the ablation experiment with the approximate image viewing window marked; ruler increments are 1 mm.

From the acquired images in Figure 2, an increased optoacoustic signal is clearly observed to come from the damaged tissue volume. The absorption and scattering coefficients of heat-damaged myocardial tissue have been previously reported to be higher than those from unablated tissue between 600 to 700 nm[12–14]. Assuming that the optical properties behave similarly in the near-infrared spectrum, and considering that optoacoustic signals correlate with light absorption, this supports our assumption that the region of high optoacoustic signal represents the highly-coagulated tissue of the RFA-generated lesion. The increase in absorption coefficient is hypothesized to arise from the denaturation of blood[13]. Additionally, the optoacoustic signal also depends on the Grüneisen parameter, which is a function of the thermal expansion coefficient, the speed of sound, and the heat capacity, and these parameters are also expected to change in heat-damaged tissue.

3.2 Dynamic lesion visualization

The real-time capability of the optoacoustic technique to capture the lesion formation during RFA can be observed from the sequence of images in Figure 3. The optoacoustic images depicting the time evolution of the lesion presumably convey two main effects: (1) optical property changes in the ablated tissue volume and (2) temperature changes, with the

latter primarily affecting the strength of the measured optoacoustic signals due to an increase in the Grueneisen parameter[15]. The effect of temperature on the optoacoustic signal is clearly observed in Figure 3 at the bottom tissue surface, where optoacoustic signal intensity increases with time as the tissue surface is slowly heated with no tissue damage occurring in this area. The temperature distribution within the tissue sample should follow a smooth continuous profile, and therefore, the sharp signal change seen in each image can still be clearly distinguished as the lesion boundary even during ablation when temperature variations are present. Speed of sound changes in the tissue can also influence the time-of-flight of the optoacoustic signals, and thus, precise location of the features in the images. However, as discussed previously in the Methods Section, these changes lead to negligible shifts in the images because the coupling medium is most certainly not affected by large temperature changes. Note that the temperature-related influences are not present in the post-ablation images in Figure 2 taken at room temperature.

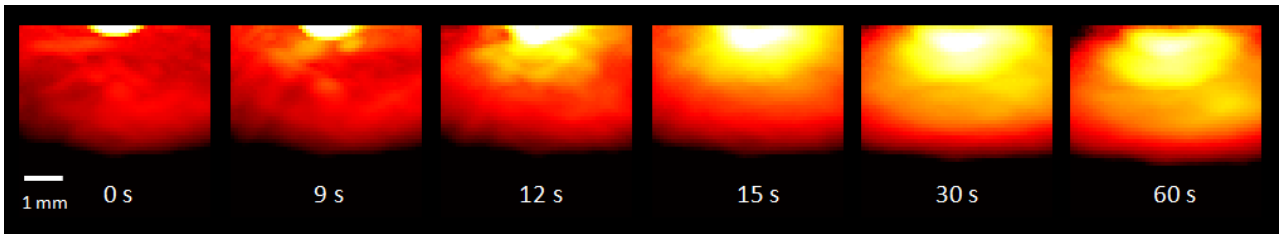

Figure 3. Time evolution of the RFA-generated lesion (same as the one shown in Figure 2) with illumination wavelength of 860 nm shown through lateral MIP planes (corrected for fluence) from the 3D-reconstructions at selected time points during the RFA heating. Scale bar representing 1 mm in all images is shown.

The depth of the lesion can be marked by the boundary of the ablated tissue volume observed in the image. One can define the leading edge of the lesion boundary as the first instance from the illumination-side surface of the tissue sample along the centerline signal where the optoacoustic signal exceeds an arbitrary threshold, in this case a 30% increase from the original signal. With this arbitrary definition of the lesion boundary, the growth of the lesion depth in time can be then automatically established from the images, as shown in Figure 4. For a short period of 10 seconds after the beginning of the RFA process, no lesion formation is observed. This is likely attributed to the tissue heating time required before a critical temperature is reached for ablation. The time that the temperature reading at the electrode tip reaches a temperature of 50°C approximately coincides with this delay, and lesion formation has been suggested to form when the tissue temperature exceeds 50°C[16]. The start of the lesion formation is then in good agreement with the heating time. The ablation process can be readily identified from the high optoacoustic contrast produced at the boundary of the highly coagulated tissue. After the lesion formation begins, the region of ablated tissue increases in size before nearly reaching a steady state value. The precise correlation between the selected threshold and the physical lesion properties is still a matter which must be calibrated based on the desired extent of damage to be detected.

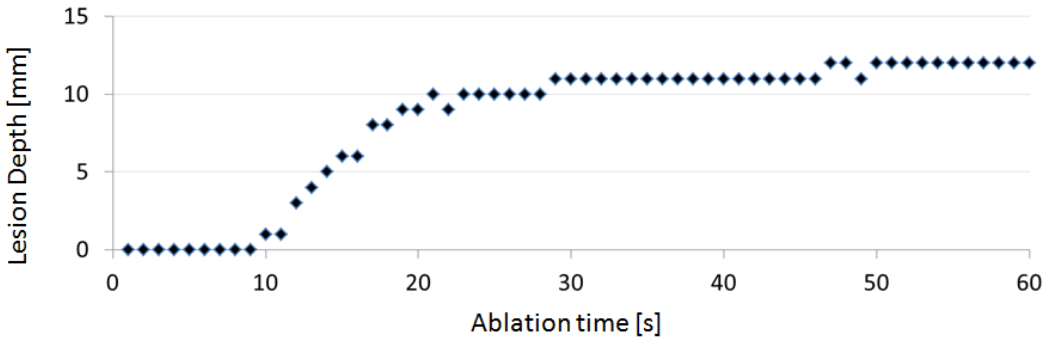

Figure 4. Progression in time of the growth of the lesion boundary during the RFA heating (same as the one shown in Figure 3), as defined by an image intensity threshold on the optoacoustic images.

4. DISCUSSION AND CONCLUSIONS

This study was performed ex vivo only using excised samples of near-homogeneous porcine ventricular myocardial tissue. Optoacoustic contrast delineating the highly coagulated tissue should also be present in ablation of in vivo atrial myocardial tissue, though the quantitative contrast may differ. Further investigations are needed to confirm the optoacoustic contrast at the lesion boundary in different types of myocardial tissue during in vivo experiments.

Many current RFA treatments are performed using saline-irrigated-tip catheters to lower the electrode and tissue surface temperature, preventing impedance rise during ablation at high power and producing deeper and larger lesions [17]. Despite the fact that the current study utilized a non-irrigated-tip catheter, one may expect the properties of the necrotic tissue formed with an irrigated-tip catheter to be similar to the current results, thus still leading to a sufficient optoacoustic contrast to clearly delineate the areas of tissue coagulation. Nevertheless, the lesion formation dynamics and the final lesion size may be different when using an irrigated tip catheter, which will also be the subject of future investigations.

The current study demonstrates that high optoacoustic contrast is observed at the boundary of the highly coagulated tissue, providing a strong motivation for modifying the current system into a clinically-applicable tool; however, the physical geometry of the optoacoustic illumination and detection system must be modified before implementation in a clinical treatment is practical. One method to achieve this, closely linked to the configuration used herein, may include optoacoustic illumination from the ablation catheter, for example either from inside the catheter center or surrounding the catheter tip, and acoustic detection from outside the body using a detector array similar to the one used in the current study. Another possibility could employ acoustic detection from within the catheter tip using micro-detector arrays or fiber-based acoustic detectors.

In conclusion, the results of the current study demonstrate that a feedback tool based on optoacoustic imaging can provide the capability of three-dimensional imaging in real time at a rate of at least 10 Hz by optoacoustic imaging using a single excitation wavelength. Higher imaging rates are readily possible if using lasers with higher repetition rates. The optoacoustic monitoring methodology carries an excellent absorption-based contrast delivering a conclusive distinction at the boundary of the highly coagulated tissue, thus providing an advantage over previously suggested ultrasound-based techniques[4,5]. The method can visualize deeper lesions than those measured with currently proposed optical techniques[7]. The main limitation on imaging depth is due to fluence decay as light propagates within tissues. In the current study sufficient penetration through tissue thicknesses of over 6 mm was shown. However, optoacoustic tomography was previously applied to image up to 15 mm in soft human tissues[10]. This study demonstrates the potential of optoacoustic monitoring to be developed into a real-time lesion monitoring feedback system that can improve the success rate of clinical RFA treatments of cardiac arrhythmia.

5. ACKNOWLEDGEMENTS

GAP acknowledges support from a University Foundation Fellowship from the Technical University of Munich. DR acknowledges support from the European Research Council under grant agreement ERC-2010-StG-260991.

REFERENCES

[1] Lloyd-Jones, D., Adams, R. J., Brown, T. M., Carnethon, M., Dai, S., De Simone, G., Ferguson, T. B., Ford, E., Furie, K., Gillespie, C., Go, A., Greenlund, K., Haase, N., Hailpern, S., Ho, P. M., Howard, V., Kissela, B., Kittner, S., Lackland, D., Lisabeth, L., Marelli, A., McDermott, M. M., Meigs, J., Mozaffarian, D., Mussolino, M., Nichol, G., Roger, V. L., Rosamond, W., Sacco, R., Sorlie, P., Stafford, R., Thom, T., Wasserthiel-Smoller, S., Wong, N. D., and Wylie-Rosett, J., "Heart disease and stroke statistics--2010 update: a report from the American Heart Association," Circulation 121(7), 46–215 (2010).

[2] Verma, A. and Natale, A., "Should atrial fibrillation ablation be considered first-line therapy for some patients? Why atrial fibrillation ablation should be considered first-line therapy for some patients," Circulation 112(8), 1214–22 (2005).

[3] Vergara, G. R., Vijayakumar, S., Kholmovski, E. G., Blauer, J. J. E., Guttman, M. A., Gloschat, C., Payne, G. Vij, K., Akoum, N. W., Daccarett, M., McGann, C. J., Macleod, R. S., and Marrouche, N. F., "Real-time magnetic resonance imaging-guided radiofrequency atrial ablation and visualization of lesion formation at 3 Tesla.," Heart Rhythm 8(2), 295–303 (2011).
[4] Wright, M., Harks, E., Deladi, S., Suijver, F., Barley, M., van Dusschoten, A., Fokkenrood, S., Zuo, F., Sacher, F., Hocini, M., Haïssaguerre, M., and Jaïs, P., "Real-time lesion assessment using a novel combined ultrasound and radiofrequency ablation catheter.," Heart Rhythm 8(2), 304–12 (2011).
[5] Eyerly, S. A., Bahnson, T. D., Koontz, J. I., Bradway, D. P., Dumont, D. M., Trahey, G. E., and Wolf, P. D., "Intracardiac acoustic radiation force impulse imaging: a novel imaging method for intraprocedural evaluation of radiofrequency ablation lesions," Heart Rhythm 9(11), 1855–62 (2012).
[6] Stephens, D. N., Truong, U. T., Nikoozadeh, A., Oralkan, Ö., Seo, C. H., Cannata, J., Dentinger, A., Thomenius, K., de la Rama, A., Nguyen, T., Lin, F., Khuri-Yakub, P., Mahajan, A., Shivkumar, K., O'Donnell, M., and Sahn, D. J., "First in vivo use of a capacitive micromachined ultrasound transducer array–based imaging and ablation catheter," J. Ultrasound Med. 31(2), 247–256 (2012).
[7] Fleming, C. P., Quan, K. J., Wang, H., Amit, G., and Rollins, A. M., "In vitro characterization of cardiac radiofrequency ablation lesions using optical coherence tomography.," Opt. Express 18(3), 3079–92 (2010).
[8] Dana, N., Di Biase, L., Natale, A., Emelianov, S., and Bouchard R., "In-vitro photoacoustic visualization of myocardial ablation lesions.," Heart Rhythm 11(1), 150-7 (2014).
[9] Laser Institute of America: American National Standard for Safe Use of Lasers ANSI Z136. 2007.
[10] Deán-Ben, X. L. and Razansky, D., "Portable spherical array probe for volumetric real-time optoacoustic imaging at centimeter- scale depths," Opt. Express 21(23), 28062-71 (2013).
[11] Deán-Ben, X. L., Buehler, A., Ntziachristos, V., and Razansky, D., "Accurate model-based reconstruction algorithm for three-dimensional optoacoustic tomography," IEEE Trans. Med. Imaging 31(10), 1922–8 (2012).
[12] Thomsen, S., Jacques, S., and Flock, S., "Microscopic correlates of macroscopic optical property changes during thermal coagulation of myocardium," SPIE Vol. 1202 Laser-Tissue Interact. 1202, 2–11 (1990).
[13] Pickering, J. W., Bosman, S., Posthumus, P., Blokland, P., Beek, J. F., and van Gemert, M. J., "Changes in the optical properties (at 632.8 nm) of slowly heated myocardiu.," Appl. Opt. 32(4), 367–71 (1993).
[14] Agah, R., Gandjbakhche, A. H., Motamedi, M., Nossal, R., and Bonner, R. F., "Dynamics of temperature dependent optical properties of tissue: dependence on thermally induced alteration," IEEE Trans. Biomed. Eng. 43(8), 839–846 (1996).
[15] Larin, K. V., Larina, I. V., Esenaliev, R. O., "Monitoring of tissue coagulation during thermotherapy using optoacoustic technique," J. Phys. D. Appl. Phys. 38, 2645–2653 (2005).
[16] Haines, D. E. and Watson, D. D., "Tissue heating during radiofrequency catheter ablation: a thermodynamic model and observations in isolated perfused and superfused canine right ventricular free wall," Pacing Clin. Electrophysiol. 12(6), 962–76 (1989).
[17] Nakagawa, H., Yamanashi, W. S., Pitha, J. V., Arruda, M., Wang, X., Ohtomo, K., Beckman, K. J., McClelland, J. H., Lazzara, R., and Jackman, W. M., "Comparison of in vivo tissue temperature profile and lesion geometry for radiofrequency ablation with a saline-irrigated electrode versus temperature control in a canine thigh muscle preparation," Circulation 91, 2264–2273 (1995).